Evidence for a pH Difference Controlled by Thermodynamics between the Interior and the Exterior of a New Type of Vesicles in Suspension

Fabienne Gauffre*,† and Didier Roux

Centre de recherche Paul Pascal, av. du doc. Schweitzer, 33600 Pessac, France

Received June 23, 1998. In Final Form: December 21, 1998

Spherical surfactant aggregates of a new type were recently discovered. Named spherulites or onions, these aggregates are droplets of lamellar phase that can also be seen as vesicles (0.1−20 μm) with a dense multilamellar structure. In this article, we report the formation of an aqueous dispersion of spherulites with a difference in acidity between the bulk phase and the vesicles. This pH difference is achieved by the addition of fatty acids to the surfactant system. A series of fatty acids of varying chain length (from acetic acid to dodecanoic acid) is studied and is shown to induce different values of the pH shift. pH shifts up to 1.5 units are measured. This pH difference is thermodynamical in nature. A theoretical description using simple thermodynamics is proposed; it is used to build up an experimental pH determination without the use of a local probe. It is demonstrated herein that spherulites are a new type of encapsulating system that permits a thermodynamical control of acidity inside the microcapsule.

Introduction

Encapsulation technology encompasses a variety of applications:[1] for example, controlled release, mixing of normally incompatible substances, retention of volatile compounds, environmental protection, and vectorization. It is employed in areas such as pharmaceuticals, the cosmetic and food industries, and agriculture, and a large number of systems are now available for encapsulation purposes. For a number of these applications acidity control inside the "microcapsule" is essential. Applications of pH-controlled microcapsules would be, for example, stabilization of various pH-sensitive compounds such as aroma and vitamins or in-vivo use of drugs unstable at a physiological pH. However, the small size of these structures often precludes the direct use of pH electrodes. Local probe techniques have been used—using pH-sensitive dyes[2,3] or fluorescent compounds[4−6]—but very few of them give absolute measurements because of the non-aqueous environment inside the microcapsule.

Here, we describe a new type of encapsulation process which, among many other advantages, can be used for "pH-controlled encapsulation". The microcapsule is a multilamellar vesicle of surfactant named "spherulite" or "onion". Spherulites are in fact droplets of lamellar phase (see below). Thus, aqueous suspensions of spherulites are diphasic systems consisting of a lamellar phase dispersed into water. A pH difference between the two phases is achieved through the addition of a fatty acid to the system. In this system, the surfactant bilayers in the lamellar phase are permeable to ions and to the fatty acid/fatty base species. Therefore, the difference in pH results from the partition of these species between the two phases and from the different dissociation of the acid in the lamellar phase and in the bulk. The nature of the fatty acid allows one to control the pH difference. Our system differs strongly from the classical case of liposomes. Indeed, in the liposomes case, a pH difference between the internal core and the bulk phase is generally created by the encapsulation of a buffer solution into an impermeable membrane. Therefore, pH control in the liposomes case is explicitly due to kinetic effects.

This paper is in three parts: first, we describe our encapsulating system, the "spherulites". Subsequently, we propose a theoretical description of acidity control in a model system consisting of microcapsules dispersed in an aqueous solution and an acidic species. This model is general and should apply not only to spherulites but also to other related systems where the pH difference is controlled by thermodynamical equilibrium. Finally, our theoretical predictions are compared with experimental observations.

Spherulites Structure and Preparation[7−9]

Spherulites are a new type of multilamellar vesicles of surfactant (Figure 1). These vesicles are formed when a pure lamellar phase (i.e., a sample situated in the one-phase lamellar region of the phase diagram) is sheared in a certain range of shear rates.[7] Under these conditions, the lamellar phase experiences an hydrodynamical transition and reorganizes in spherical or polyhedral microdomains (Figure 1).[10] These microdomains are multilamellar vesicles named "spherulites". Very little polydispersity is obtained when an homogeneous shear is applied using a homemade shear cell and the size of the vesicles

* To whom correspondence should be addressed.

† Present address: LCC, 205 rte de Narbonne, 31077 Toulouse Cedex, France.

(1) Gregoriadis, G. In *Liposomes as Carriers of Drugs*; Wiley and Sons: New York, 1988; Lasic, D. *Am. Sci.* **1992**, *80*, 20−31; Lopez-Berenstein, G.; Fidler, I. In *Liposomes in the Therapy of Infectious Desease and Cancer*; Liss: New York, 1989.

(2) Rossignol, M.; Thomas, P.; Grignon, C. *Biochim. Biophys. Acta* **1982**, *684*, 195−199.

(3) Mukerjee, P.; Banerjee, K. *J. Phys. Chem.* **1964**, *68* (12), 3567−3574.

(4) Bardez, E.; Monnier, E.; Valeur, B. *J. Colloid Interface Sci.* **1985**, *112* (1), 200−207.

(5) Bardez, E.; Goguillon, B.; Keh, E.; Valeur, B. *J. Phys. Chem.* **1984**, *88*, 1909−1913.

(6) Bramhall, J. *Biochemistry* **1986**, *25*, 3958−3962.

(7) Diat, O.; Roux, D.; Nallet, F. *J. Phys. II (France)* **1993**, *3*, 1427−1452.

(8) Diat, O.; Roux, D. *J. Phys. II (France)* **1993**, *3*, 9−14.

(9) Roux, D.; Diat, O. French Patent No. 92 04108.

(10) Gulik-Krzywicki, T.; Dedieu, J.; Roux, D.; Degert, C.; Laversanne, R. *Langmuir* **1996**, *12* (20), 4668−4671.

10.1021/la980734d CCC: $18.00
Published on Web 04/06/1999

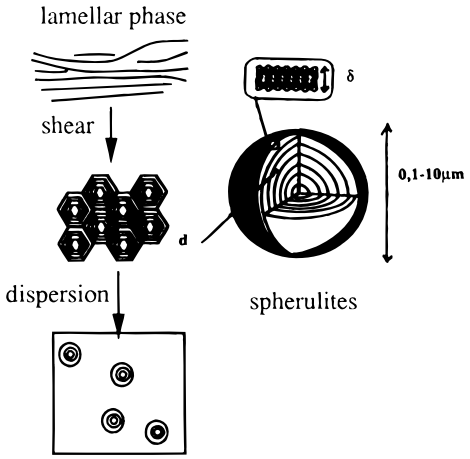

Figure 1. Spherulites structure and preparation. Spherulites are produced by applying a controlled shear to a lamellar phase of surfactant. The resulting vesicle-like microdomains are multilamellar vesicles of surfactant made of a regular stacking of surfactant bilayers separated by water layers. Compacted spherulites can be dispersed by adding an excess amount of solvent to the sheared lamellar phase. The interlamellar distance between two consecutive layers and the bilayer thickness are typically $d = 50-200$ Å and $\delta = 30-50$ Å.

has been shown to vary as the inverse of the square root of the shear rate.[7] Sizes ranging from 0.1 to 20 μm are obtained depending upon the lamellar-phase composition and upon the shear rate. Aqueous dispersion of spherulites are obtained by diluting the compact phase of spherulites into water (Figure 1).

Spherulites are well-suited for encapsulation purposes. Encapsulation is achieved simply by incorporating the desired compound, hydrophilic or hydrophobic, in the lamellar phase before applying the shear to produce spherulites. This particular encapsulation process is less severe when compared to processes of encapsulation into "classical" liposomes. This allows encapsulation of fragile biological materials. A wide variety of compounds such as fluorescent dyes,[11] copper salts,[12] enzymes,[13] and oligonucleotides have already been encapsulated in spherulites with an encapsulation ratio (i.e., the amount of encapsulated product over the global amount involved in the process) of greater than 80%. A large number of surfactant systems—neutral, cationic, and anionic—have already been formulated to produce spherulites.

In the present study, a neutral lamellar phase has been prepared using the zwitterionic soybean lecithin mixed with a nonionic cosurfactant (C12E5) and fatty acids of various chain lengths ($H-(CH_2)_{n-1}-COOH$, $n = 2, ..., 12$). The aim of using fatty acids was to induce varying acidity within the spherulites. Indeed, acids of different chain lengths were expected to have different affinities for the membrane and consequently to lead to different pH effects. When the acid-containing spherulites are dispersed into an aqueous solution, the basic and acidic species freely distribute between the water phase and the spherulites.

Spherulites can be considered as droplets of lamellar phase. It is an emulsion made of a lamellar phase dispersed into water. Thus, our experimental system simply consists of an acid/base couple exchanging between two phases: water and a dispersed lamellar phase. To determine an experimental way of studying the pH difference between the lamellar droplets and outside, we need to first model the effect. This system will be modeled in the following section, using only classical acid/base chemical equilibria and partition coefficients.

(11) Milner, S.; Gauffre, F.; Roux, D. In preparation.
(12) Gauffre, F.; Roux, D. Submitted to Langmuir.
(13) Bernheim, A.; Ugazio, S.; Gauffre, F.; Viratelle, O.; Roux, D. In preparation.

Model

Now, we propose a thermodynamical description of our system, consisting of droplets of lamellar phase dispersed into water together with an acid/base couple distributing freely between the two phases. This description can be applied to many other systems, for example, aqueous dispersions of gel particles. In the case of gel particle dispersions, acid molecules can adsorb on the polymeric chains of the gel or stand in the bulk water phase. However, in the spherulites case, when chemical equilibrium is reached, all chemical species are distributed between the bulk water phase and the spherulites as demonstrated in the Experimental Section. Inside the spherulites, molecules can be inserted into surfactant bilayers or situated in the water layers. This depends primarily on the length of the aliphatic chain.

The following theoretical analysis allows us to determine the parameters that control acidity in each phase, and consequently to elaborate on an experimental process in order to determine the pH inside the spherulites.

We emphasize here that the surfactant system is neutral and that the acid concentration in the spherulites was kept under 0.5 M (see Experimental Section). Moreover, we checked experimentally that varying the acid concentration, and hence the charge concentration, in the system does not affect our results.[14] Thus, electrostatic effects are neglected in the theoretical treatment.

Three main hypotheses are assumed: (1) All chemical equilibria are attained. (2) Distribution of the acid (AH) and basic (A^-) forms between the two phases can be described in terms of partition coefficients. The partition coefficients for the acid (k_a) and the base (k_b) form will be written as follows:

$$k_a = \frac{[AH]_i}{[AH]_o} \quad \text{(a) and } k_b = \frac{[A^-]_i}{[A^-]_o} \quad \text{(b)} \qquad (1)$$

where the index "i" or "o" refers to values *inside* and *outside* the spherulites, respectively. (3) Acid dissociation in both phases can be described using dissociation constants that are a priori different. For instance, in the case of acid molecules inserted in spherulites bilayers, even though the polar headgroups are in contact with water, they experience a microscopic environment very different from that in pure water.

Acidity constants in the bulk phase (K_o) and in the dispersed phase (K_i) are written

$$K_o = \frac{[A^-]_o[H^+]_o}{[AH]_o} \quad \text{(a) and } K_i = \frac{[A^-]_i[H^+]_i}{[AH]_i} \quad \text{(b)} \qquad (2)$$

These chemical equilibria are schematically represented in Figure 2.

Concentrations are used in place of activities because, as mentioned before, we used neutral lamellar phases and low acid concentrations. However, by using activities and electrochemical potentials, this model can be generalized to higher concentrations and to cationic and anionic systems.

Although lamellar phases are heterogeneous at microscopic scale, they are thermodynamical phases. Therefore,

(14) Gauffre, F. Thesis, Université Bordeaux I, France, 1997.

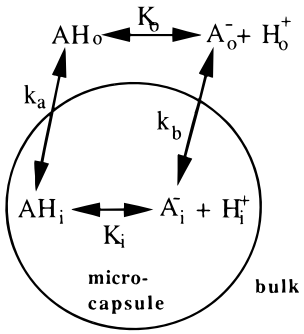

Figure 2. Schematic representation of the four equilibria-controlling concentrations of the acidic (AH) and basic (A^-) forms of an acid species in the two phases. Partition coefficients between the microcapsules and the bulk phase are k_a and k_b, respectively; dissociation constants in the bulk phase and the microcapsules are K_o and K_i, respectively.

the "classical" use of partition coefficients and of chemical reaction equilibria are still valid. However, concentrations in the spherulites ([ ]$_i$) are mean concentrations, and thus this model gives no information about the microscopic partitioning of chemical species inside the spherulites.

Combining eqs 1 and 2 leads to

$$\frac{[H^+]_i}{[H^+]_o} = \frac{K_i k_a}{K_o k_b} \tag{3}$$

hence

$$\Delta pH = pH_i - pH_o = -\log(\beta) \tag{4}$$

where

$$\beta = \frac{K_i k_a}{K_o k_b}$$

This relation expresses the existence of a shift of pH between the dispersed phase and the bulk phase. This shift depends on the values of the acidity constants K_o and K_i and of the partition coefficients k_a and k_b. Note that $k_a > k_b$ tends to create an "acid shift" ($\beta > 1$, i.e., the microcapsule is more acid than the bulk phase). This is the case in the present experimental system as the basic forms, charged, of fatty acids are more soluble in water than the corresponding acidic forms, uncharged, as excepted for acids with shorter chain lengths as will be seen later on. Furthermore, the acidity constant ratio is in favor of an acid shift when $K_i > K_o$ (i.e., the acid is more dissociated in the microcapsules than in the bulk phase). We shortly will see that fatty acids are in fact less dissociated in the lamellar phase than in water. Thus, the resulting pH shift will depend on the competition between the two ratio.

Now, we express pH_o—which can be directly measured—as a function of the total concentration in fatty acid (both AH and A^- forms) within the system. This results from the following equations of conservation:

(1) The total number of A groups (AH and A^-) is constant; hence,

$$C(V_i + V_o) = [A^-]_i V_i + [A^-]_o V_o + [AH]_i V_i + [AH]_o V_o$$

where C is the global concentration in A groups, V_o the aqueous solution volume (without capsules), and V_i the internal volume (for instance, total spherulites volume in the spherulite case).

(2) The global system remains electrically neutral, then we have

$$[H^+]_i V_i + [H^+]_o V_o = ([A^-]_i + [OH^-]_i)V_i + ([A^-]_o + [OH^-]_o)V_o$$

When AH is present, it provides hydronium ions (H_3O^+) that greatly outnumber any OH^- that stem from water autoprotolysis. Hence, it is reasonable to neglect the OH^- concentration in writing electrical neutrality:

$$[H^+]_i V_i + [H^+]_o V_o = [A^-]_i V_i + [A^-]_o V_o$$

Consequently, we bring all these features together in order to express $[H^+]_o$ which is experimentally determined through pH measurement of the bulk phase in terms of known or experimentally available parameters.

If we express the two conservation conditions in terms of external concentrations alone by using partition coefficients, it yields

$$C(1 + w) = [A^-]_o(1 + k_b w) + [AH]_o(1 + k_a w)$$

and

$$[H^+]_o(1 + \beta w) = [A^-]_o(1 + k_b w)$$

where $w = V_i/V_o$.

The conservation of A groups can be expressed in terms of $[A^-]_o$ alone by making use of the acidity constant K_o:

$$[A^-]_o = \frac{C(1 + w)}{(1 + k_w w) + \frac{[H^+]_o}{K}(1 + k_a w)} \tag{5}$$

the electrical neutrality condition then becomes

$$C = \frac{[H^+]_o^2}{K_o}\frac{(1 + bw)}{(1 + w)}\frac{1 + k_a w}{(1 + k_b w)} + [H^+]_o\frac{(1 + bw)}{(1 + w)} \tag{6}$$

Solving this second-order equation gives a unique positive solution:

$$[H^+]_o = \frac{-K_o\left(\frac{C^*}{C} - 1 + k_b\right)}{2\left(\frac{C^*}{C} - 1 + k_a\right)} + \frac{1}{2}\left[\frac{\left(\frac{C^*}{C} - 1 + k_b\right)^2}{\left(\frac{C^*}{C} - 1 + k_a\right)^2}K_o^2 + \frac{4C^*K_o}{\left(\frac{C^*}{C} - 1 + \beta\right)}\frac{\left(\frac{C^*}{C} - 1 + k_b\right)}{\left(\frac{C^*}{C} - 1 + k_a\right)}\right]^{1/2} \tag{7}$$

where $C^*/C = 1/w + 1$ (i.e., C^* would be equal to $[A]_i$ if all A groups where in the internal phase). Hence, the pH of the bulk phase (pH_o) is related to eq 7 through the partition and acidity constants, and to w and C that are explicitly chosen.

By taking $k_a = k_b$ and $K_o = K_i = K$, we can recover the equivalent relation for an acid (with acidity constant K) in water. Indeed, eq 3 gives $[H^+]_o = [H^+]_i = [H^+]$ and eq 6 becomes

$$C = \frac{[H^+]^2}{K} + [H^+] \tag{8}$$

which has a unique positive solution

$$[H^+] = \frac{1}{2}[-K + (K^2 + 4CK)^{1/2}] \quad (9)$$

In the case of a weak acid ($[H^+] \ll C$) eq 8 rearranges into the well-known expression: $pH = 1/2(pK - \log C)$.

Considering eq 7, concentration C can be experimentally varied in two ways in the spherulites case. (1) Starting from spherulites containing an initial concentration of acid C^*, an increasing amount of these spherulites are dispersed into water to increase the global concentration in acid C (i.e., C^* is constant whereas w increases). Note that in this case the maximum global concentration is $C = C^*$ which corresponds to a bulk volume equal to 0. (2) An increasing amount of acid is added to a dispersion containing a fixed volume of spherulites (i.e., C^* increases whereas w remains constant). In the latter case, by taking

$$K = K_o(1 + wk_b)/(1 + wk_a) \quad \text{and}$$
$$C' = C(1 + w)/(1 + wb)$$

Equation 6 rearranges in the form of eq 8. Therefore, pH values in the bulk will be the same as those for an acid species of acidity constant K in water, at concentration C'.

Evolution of pH_o (thick line) and pH_i (thin lines) values with global concentration C in the former case is simulated in Figure 3 with two different sets of values: (a) $C^* = 1$ M; $pK_o = 4$; $pK_i = 7$; $k_a = 2.10^5$; $k_b = 10$. (b) $C^* = 1$ M; $pK_o = pK_i = 4$; $k_a = 120$; $k_b = 10$. In both cases pH_o and pH_i curves are parallel as expected from eq 4. At weak concentrations (high dilution of spherulites), pH_o is the same as that for an acid of $pK = pK_o$ at the same concentration in water (thick dashed lines). Indeed, for $w \rightarrow 0$ eq 6 rearranges in the form of eq 9 to give $C = ([H^+]_o)^2/K_o + [H^+]_o$. This arises because the amount of acid remaining in highly diluted spherulites is much weaker than that in the bulk phase. In a symmetrical way, at high concentrations (spherulites dispersed in a weak amount of water), the pH_i is the same as that for an acid of $pK = pK_i$ in water (thin dashed lines). Indeed, for $w \rightarrow \infty$, eq 6 rearranges in $C = ([H^+]_i)^2/K_i + [H^+]_i$.

We see that the same behavior is expected for $pH_o = f(C)$ at a high dispersion ratio and for $pH_i = f(C)$ at a low dispersion ratio. As these two curves are parallel, this reflects that the dilution of spherulites corresponds to going from one behavior to the other. The interesting fact is that $pH_o = f(C)$ contains a lot of information because of this crossover.

In conclusion, this model allows us to determine ΔpH. Although pH_o is simply measured with a classical pH electrode dropped in the bulk phase, no direct determination of pH_i (in the spherulites) is available. However, the acidity constant in water (K_o) and the partition coefficients (k_b and k_a) are easily determined. Consequently, eq 7 allows us to determine values for K_i by simply fitting the experimental curve in Figure 3 with K_i being the only unknown parameter (recall that $\beta = K_i k_a/K_o k_b$).

Results and Discussion

We systematically determined the four constants k_a, k_b, K_o, and K_i for the fatty acids $H-(CH_2)_{n-1}-COOH$ ($n = 2, \ldots, 12$) as follows.

(a) Partition Coefficient Measurements. Starting from a global concentration C, we adjusted the pH conditions in order to have predominantly either the basic or the acidic form. Spherulites were then separated from the bulk phase, either by centrifugation or by dialysis experiments, and bulk phases were titrated. Values for k_a and k_b are then calculated from

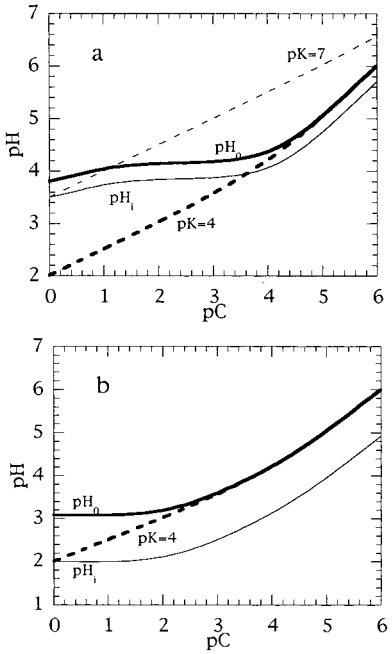

Figure 3. Theoretical prediction for pH value in the bulk (pH_o, thick solid line) and in the internal phase (pH_i, thin solid line) as a function of the mean concentration C, expressed in pC units ($pC = -\log(C)$). Two different cases: (a) $C^* = 1$ M; $pK_o = 4$; $pK_i = 7$; $k_a = 2 \times 10^5$; $k_b = 10$. (b) $C^* = 1$ M; $pK_o = pK_i = 4$; $k_a = 120$; $k_b = 10$. Dashed lines represent theoretical pH values in an aqueous solution of an acid as a function of its concentration C (corresponding pK values are indicated on the graphs).

$$k_a = (C(V_i + V_o) - V_o[AH]_o)/(V_i[AH]_o) \quad \text{and}$$
$$k_b = (C(V_i + V_o) - V_o[A^-]_o)/(V_i[A^-]_o)$$

Experimental Procedure. Starting from a spherulites dispersion with a mean concentration of acid C, the experimental procedure follows three steps.

(1) Converting all A form in A^- or AH respectively to enable k_a and k_b determination. For k_b measurements, AH is converted to A^- form by adding 1.2 equiv of NaOH to the spherulites dispersion. For k_a measurements there is no need to add any acid as long as $pH < pK$.

(2) Separation of the spherulites from the bulk water phase. Spherulites separation was performed by centrifugation when possible. However, in certain cases the density of acid containing spherulites did not allow an effective separation by centrifugation. Spherulites separation was then performed by dialysis experiments (see Experimental Section). It was verified that both methods give similar results. The influence of the dispersion ratio also proved to be negligible.

(3) Titration of the bulk phase by conductometric titration (see Experimental Section). Concentration in the spherulites is then deduced from the mean concentration and the titrated concentration in the bulk. Partition coefficients are then directly obtained from eq 1.

Results. Figure 4 displays experimental values for k_a and k_b. k_a for dodecanoic acid could not be determined because of its sparing solubility in the water phase. In the case of acetic to butanoic acids, k_b could not be determined because concentration in the spherulites was too weak to be estimated. Both k_a and k_b values increase with the chain length, indicating, as expected, increasing affinity for the membrane when their hydrophobic part increases. Furthermore, we always measured higher values for k_a than for the corresponding k_b, which accounts for the

greatest solubility of the charged form A^- in water. We see in Figure 4 that $\log(k_a)$ and $\log(k_b)$ linearly increase with n. The corresponding best fits give

$$\log(k_a) = 0.51n - 1.64 \quad \text{and} \quad \log(k_b) = 0.23n - 0.16$$

We observe that the slope for k_b is smaller than for k_a in a ratio equal to about 2. This result can be interpreted as arising from the difference in entropy to transfer one single molecule (AH) or two ions (A^- and Na^+) from one phase to the other, respectively. Indeed, if a single species can distribute freely between two phases of volume V_1 and V_2, the free energy for the N_i molecules in phase i ($i = 1, 2$) is

$$F_i = N_i k_B T \ln\left(\frac{N_i \nu}{V_i}\right) + N_i u_i \qquad i = \{1, 2\}$$

The term proportional to $k_B T$ corresponds to the entropic part of the free energy, v being the molecular volume of the solute species. The term $N_i u_i$ represents the energy to bring N_i molecules from vacuum to phase i. Equality of the solute chemical potential between phase 1 and 2 immediately leads to

$$\mu_1 = \frac{\partial F_1}{\partial N_1} = k_B T\left(1 + \ln\left(\frac{N_1 \nu}{V_1}\right)\right) + u_1 = k_B T\left(1 + \ln\left(\frac{N_2 \nu}{V_2}\right)\right) + u_2 = \frac{\partial F_2}{\partial N_2} = \mu_2$$

and hence the value of the partition coefficient

$$k = \frac{\left(\frac{N_2}{V_2}\right)}{\left(\frac{N_1}{V_1}\right)} = \exp\left(-\frac{u_2 - u_1}{k_B T}\right)$$

In the case of a fatty acid molecule $H-(CH_2)_{n-1}-COOH$ it seems reasonable to assume that the energy term can be written as $u_2 - u_1 = \Delta u(n) = \Delta u_{pol} + n\Delta u_{Me}$ where Δu_{pol} is the energy difference associated with the polar headgroup whereas Δu_{Me} corresponds to the energy difference for one methyl group of the aliphatic chain.

Hence,

$$\log(k_a) = -\frac{\Delta u_{pol} + n\Delta u_{Me}}{2.3 k_B T}$$

In the case of an ion pair, both ions contribute to the free energy in phase i

$$F_i = N_i k_B T \ln\left(\frac{N_i \nu^+}{V_i}\right) + N_i u_i^+ + N_i k_B T \ln\left(\frac{N_i \nu^-}{V_i}\right) + N_i u_i^- \qquad i = \{1, 2\}$$

Equality of the chemical potential then leads to

$$k = \frac{\left(\frac{N_2}{V_2}\right)}{\left(\frac{N_1}{V_1}\right)} = \exp\left(-\frac{(u_2+ + u_2^-) - (u_1^+ + u_1^-)}{2 k_B T}\right)$$

As the internal counterions (Na^+) probably stand in the water layers of spherulites, it seems reasonable to assume that they have the same energy inside the spherulites and in the bulk water phase (i.e., $u_1^+ = u_2^+$). Thus, by writing the energy term as before,

$$u_2^- - u_1^- = \Delta u(n) = \Delta u_{pol}^- + n\Delta u_{Me}$$

we have

$$\log(k_b) = -\frac{1}{2}\frac{\Delta u_{pol}^- + n\Delta u_{Me}}{2.3 k_B T}$$

Thus, in both the case of the acidic and the basic forms, a linear curve is expected with a ratio in the slopes of the order of 2. This is because the chemical potential gain due to the $-CH_2-$ group should be the same whenever AH is dissociated or not. The experimental ratio extracted from the curve is 2.25. Values for Δu_{pol}, Δu_{pol}^-, and Δu_{Me} can also be extracted from experimental curves, we obtain

$$\Delta u_{pol} = -3.8 k_B T; \qquad \Delta u_{pol} = 0.37 k_B T \quad \text{and} \quad \Delta u_{Me} = 1.17 k_B T$$

Δu_{Me} values are in good agreement with values previously cited by Israelachvili[15] for transfer of surfactant molecules from water to a liquid phase ($\Delta u_{Me} = 1.9 K_B T$).

(b) Acidity Constants. K_o values (acidity constants in water) are obtained from the literature.[16] For $n = 2$, ..., 9 those values are well-fitted by a straight line (Figure 8) of equation $pK_o = 4.697 + 0.027n$ (eq 10), and in the following we will extrapolate K_o values for longer chain acids from this equation. Practically, pK_o has a very weak dependence on n.

Acidity constants in the spherulites were determined by means of eq 7 (vide supra). First, spherulites were formed from a pure lamellar phase containing one fatty acid at concentration C^*. Then, different dispersions were prepared by diluting those spherulites into water, to obtain different values of the global concentration C. K_i was then fitted to the experimental curve pH_o versus C, using eq 7. K_i is the only free parameter in the fit, k_a, k_b being fixed to their experimental values and K_o being obtained from eq 10.

The knowledge of k_a, k_b, K_i, and K_o, immediately gives the value for ΔpH through eq 4.

In addition to ΔpH determination, fitting the experimental curves pH_o versus C allows one to test the validity of our model and especially the approximation that identifies activities and concentrations.

Experimental Procedure. As outlined in the theoretical section, K_i values can be obtained from the experimental dilution laws $pH_o = f(C)$. Spherulites containing acid at concentration C^* were prepared by shearing a lamellar phase with no excess solvent. Then, with variation in the volumic ratio $w = V_i/V_o$ into the dispersion, different mean concentrations in acid were obtained as $C = C^*/(w + 1)$. After equilibrium is reached, the pH_o was simply measured in the bulk phase with a classic pH electrode. K_i was then determined by numerical adjustments to the experimental curve using eq 6.

Kinetics Features. Our model assumes that chemical equilibrium is reached in the system. Separation experiments did not allow us to measure acid leakage from spherulites at short times as the time necessary to work out separation was at least 4 h. However, we could

(15) Israelachvili, J. *Intermolecular and Surface Forces*; Academic Press: London, 1992.

(16) In *Handbook of Chemistry and Physics*, 48th ed.; CRC Press: Boca Raton, FL, 1967−1968.

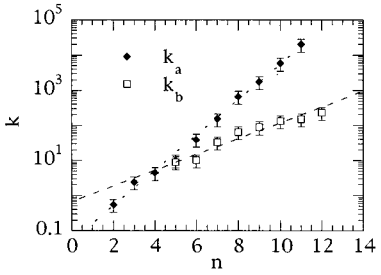

Figure 4. Experimental values of the partition coefficients between the bulk phase and the spherulites for the acidic (diamonds) and the basic (square) forms of fatty acids $H-(CH2)_{n-1}-COOH$, as a function of the chain length n.

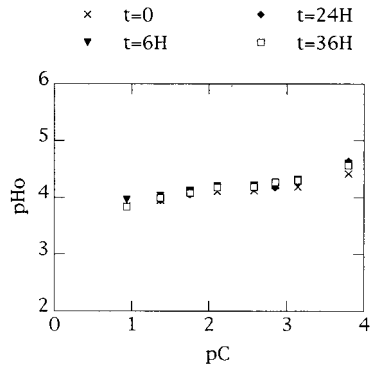

Figure 5. Kinetic evolution of the experimental curve pH_o vs pC for nonanoic acid. $t = 0$ is set at the end of the dispersion (dispersion time=30 min).

investigate the kinetic evolution of the system by measuring pH_o along a dilution curve at different times after dispersion (Figure 5). No noticeable evolution could be observed up to 36 h after dispersion. Note that the dispersion stage itself takes about 30 min.

Experimental dilution laws are displayed in Figure 6. When possible, comparison is made with the dilution law for the corresponding acid in water. Clearly, it appears that the difference between the encapsulated and the nonencapsulated cases increases with increasing chain length of the acid starting from superimposed curves for $n = 2$. Indeed, the shortest acids have weak k_a and k_b values, and are consequently mainly present in the bulk water phase. The amount of encapsulated acid is negligible; thus, pH_o is simply the pH of an aqueous solution of concentration C. Dodecanoic acid exhibits an approximately linear dilution law; k_a and k_b being over 100, encapsulated dodecanoic acid is predominant. Thus, the spherulites dispersion is equivalent to an aqueous phase containing only one type of acid: the membrane-inserted dodecanoic acid (pK = pK). pK_i can be deduced from the value at pC = 0: $^1/_2$pK_i = 3.5; hence, pK_i = 7. This qualitative result shows that the pK of membrane-inserted dodecanoic acid is 2 units higher than that for fatty acids in water (approximately 5).

Note that the superimposed curves obtained for acetic acid show that the presence of phospholipids does not influence the pH determination. Indeed, in the case of very short chain length the acid is not encapsulated and it is obvious that the pH measurements in the presence or in the absence of phospholipidic spherulites is equivalent.

All experimental dilution curves exhibit a shape identical to, or to a limited portion of, the same curve. In Figure 3a parameters were chosen to exhibit this general curve as a whole in the pC = 0−6 range. The linear behavior of acetic acid ($n = 2$) corresponds to low concentrations (pC → 5) in Figure 3a. Intermediate acids show a more extended portion of this curve with a plateau at high concentration (n = 4−8). The experimental behavior of acids with the longest chain lengths eventually resembles the high-concentration part of Figure 3a (see $n = 12$).

pK_i values are extracted from the best fits of dilution curves using eq 7 and are reported in Figure 8. The shortest acids up to $n = 8$ have pK_i values close to 4.5, while the longer acids ($n > 9$) have much higher pK_i values, close to 7.2. Nonanoic acid seems to have an intermediate behavior. Uncertainties on pK_i determination is illustrated in Figure 7 by giving slightly different values to pK_i in the theoretical curves for $n = 6$ and $n = 11$. Uncertainties are weak compared to the gap (more than 2.5 pH units) between pK values for $n < 8$ and $n > 10$. However, with regards to uncertainties the slight differences observed in Figure 8 between the shortest acids (p$K_i \approx 4-5$ for $n < 9$) or between the longest ones (p$K_i \approx 7$ for $n > 9$) can be considered as not significant.

The difference in pK_i values for short and long fatty acids is attributed to a different localization in the spherulites. Indeed, the longer acids are more likely to be inserted in the surfactant bilayers and consequently to have a different local environment than the shorter acids. Moreover, if acids are inserted in the bilayers, local concentration in ionizable groups might be high enough to induce an electrostatic inhibition of dissociation, hence an increase in the pK_i value. Note that, in this case, our assumption to neglect any electrostatic effect in pH determination remains valid, assuming there is little dissociation.

(c) ΔpH Determination. ΔpH is calculated from eq 4 using experimental values for k_a, k_b, and K_i. Results are displayed in Figure 9, showing a nonmonotonic curve with a maximum for $n = 8$, where ΔpH = 1.5 units. Indeed, the ratio k_a/k_b and K_i/K_o follows opposite evolution as n increases. One can summarize the ΔpH behavior as follows: when the length of the aliphatic chain increases, k_a/k_b increases; however, at $n = 9$ the internal pK changes suddenly and no more dissociation is expected in the spherulites (p$K_i \approx 7$) whereas AH remains relatively acidic in the bulk (p$K_o \approx 4.8$).

Experimental Section

Materials. Lamellar phases consisted of a mixture of 90% pure phosphatydylcholine extracted from soybean (Phospholipon 90, Rhône Poulenc Rörer), C12E5 (Lauropal 4, Witco), and water. All fatty acids were purchased from Aldrich. Acid-containing lamellar phases were prepared by mixing the chosen fatty acid with all other components. Dodecanoic acid is solid at room temperature and was dissolved in C12E5 prior to adding the other components. Lamellar phases compositions are given in Table 1. The acid:phospholipid molar ratio was kept constant. When equilibrium was reached, lamellar phases were sheared by a vigorous manual shear for approximately 10 min. Spherulite dispersion was performed by carefully adding a small amount of water with gentle stirring.

***k*$_b$ Measurements.** Spherulites were dispersed with 4 unit volumes of water. For acids with the shortest chain lengths ($n < 7$) the previous dispersions were diluted 50 times. After 4 h, the resulting dispersion was ultracentrifuged for 3 h at 40 000 rpm. For all other acids ($n \geq 7$), the concentrated dispersion was dialyzed overnight with 50 times its volume in an aqueous NaOH solution. In both cases, concentration of the NaOH solution was calculated to have 1.2 equiv of NaOH. After separation, concentration of A^- in the bulk phase was determined by conductometric titration using HCl.

***k*$_b$ Measurements.** For the shortest acids, spherulites were dispersed 200 times and then centrifuged as before. For $n > 5$, spherulites were dispersed 10 times and dialysis experiments

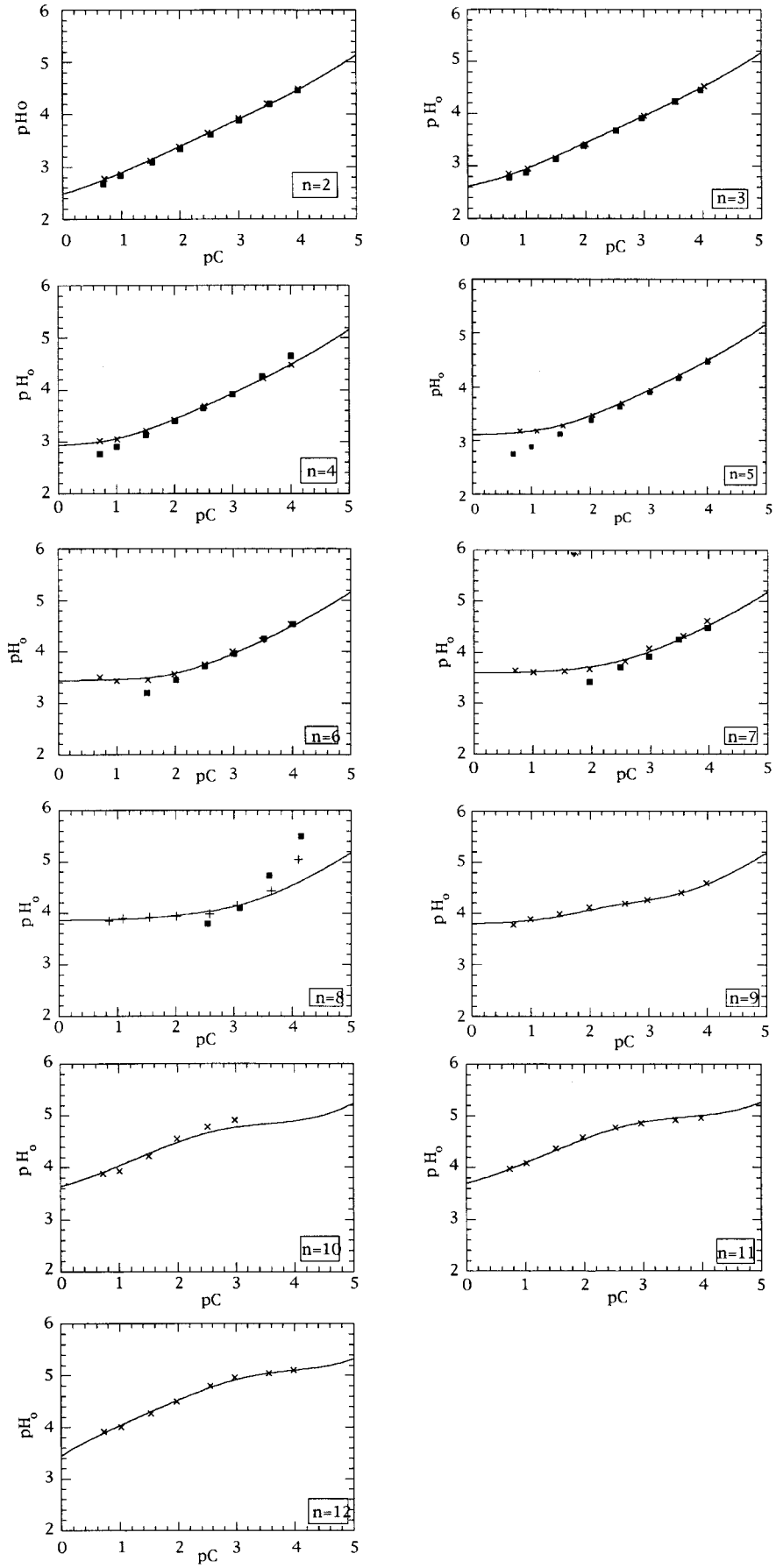

Figure 6. Crosses: pH_o measurements versus fatty acid mean concentration *C* expressed in p*C* units, for fatty acids $H-(CH_2)_{n-1}-COOH$ ($n = 2, ..., 12$). Best fits for experimental values are represented by full lines. Dots: pH measurements in aqueous solutions of the same acid. Reference curves are limited by the corresponding acid solubility in water.

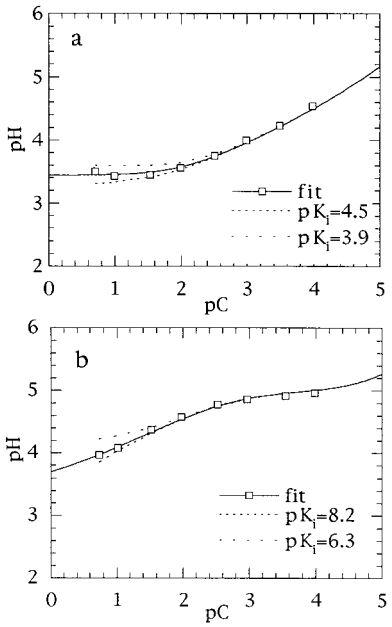

Figure 7. Uncertainties on pK_i values as determined by fitting experimental dilution curves for $n = 6$ and $n = 11$. Squares: experimental data. Full line: best fit. Dashed lines: theoretical curves with modified pK_i values with all other parameters unchanged.

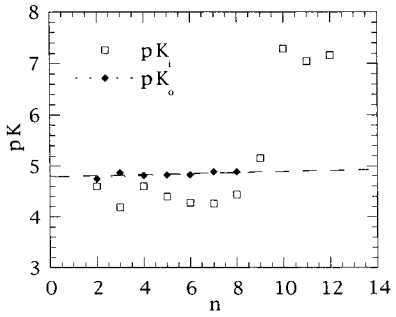

Figure 8. pK values in the bulk and in the spherulites for fatty acids H−$(CH_2)_{n-1}$−COOH vs n.

were run in 20 times the same volume. After separation, the bulk phase was titrated by NaOH.

Dialysis membranes (molecular weight cutoff: 100 000) were obtained from Spectra Por. Prior to dialysis experiments, membranes were saturated with fatty acid by dipping the membrane overnight in an aqueous acid solution of the same concentration. The saturated membranes were then washed with water before use.

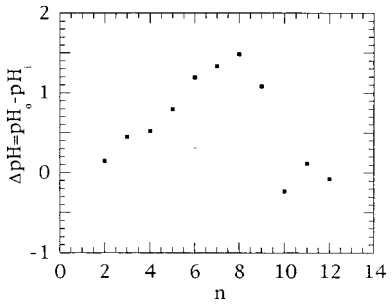

Figure 9. Values of pH difference between the bulk and the spherulites for fatty acids H−$(CH_2)_{n-1}$−COOH vs n.

Table 1. Lamellar-Phase Composition in Weight Percentages, pK_o Values (Extracted from Reference 16) and Experimental Values for k_a, k_b, and PK_i[a]

n	Macid (%)	MSP C (%)	pk_a	pk_b	pK_o	pK_i
2	3.4	39.6	1.5	1.5	4.75	4.6
3	4.2	38.8	2.1	3.6	4.9	4.2
4	4.5	38.5	5.5	2.7	4.8	4.6
5	5.2	37.8	10	4.2	4.8	4.4
6	5.8	37.2	27	6.2	4.8	4.3
7	6.5	36.5	153	30	4.9	4.25
8	7.1	35.9	594	55	4.9	4.4
9	7.5	35.5	1752	88	4.9	5.15
10	8.1	34.8	29000	200	4.9	7.3
11	8.6	34.4	55000	300	4.9	7.0
12	9.1	33.9	94000	600	4.9	7.15

[a] The acid and soybean phosphatidyl choline (SPC) weight percentages in the lamellar phase are indicated in the table for each fatty acid. The water and cosurfactant ratio were kept constant to the following values: water, 48%; C12E5, 9%.

Conclusion

In this paper we have presented a new system designed for pH-controlled encapsulation. Significant pH shifts between the bulk and the microcapsules have been obtained, and it was established that this shift can be tuned by an appropriate choice of acid to regulate the system. The thermodynamical description of the process of acidity control is validated by experiments. It also allows one to carry out an original experimental procedure for intravesicular pH determination without the use of a local probe.

Acknowledgment. The authors thank F. Delfosse for his help in performing the experiments.

LA980734D